JP7.5 ON LINEAR AND NONLINEAR BAROTROPIC TROPIC INSTABILITY WAVES

Cheng Zhou* and John P. Boyd
Department of Atmospheric, Oceanic and Space Sciences, University of Michigan, Ann Arbor, MI 48109-2143

1. INTRODUCTION

Tropical instability waves (TIWs) or equatorial long waves have been extensively studied over last three decades. These westward propagating oscillations of equatorial currents were first detected in current meter records as meanderings of the South Equatorial Current(SEC) in the Atlantic ocean by Duing et al. (1975) and in satellite infrared images as cusplike deformations of North Equatorial Front (NEF) in the Pacific ocean by Legckis(1977). They were subsequently identified in various observations, including in situ and remote satellite measurements of velocity (Halpern et al., 1988; Qiao and Weisberg, 1995), in situ measured temperature (Lyman et al.,2007), satellite measured sea surface temperature (Chelton et al., 2000, 2001), surface dynamic height (Miller et al., 1985), surface wind (Chelton et al., 2001), as well as sea colors(Jochum et al., 2004). These measurements gave various wavelengths, and periods, in ranges of 600-2000km and 16-40 days, respectively. Qiao and Weisberg (1995) gives a summary of such variations in its Table 1.

These TIWs generally fall to two categories. One appears near the equator, has a period of about 17-23 days, and is most prominent in meridional velocity. The second one is centered about 5°N, has a period around one month, and has been observed in sea surface height (SSH), sea surface temperature (SST), and velocity. Flament et al. (1996) and Kennan and Flament (2000) observed two drastically different propagation speeds of TIWs along the the equator (0.8 m/s) and along 4.5°N (0.3 m/s). They suggested these are two distinct phenomena. Lyman et al. (2007) also observed two different types of TIWs existing in the Pacific Ocean, unstable Rossby waves at a period of about 33 days characterized by subsurface temperature at 5°N and Yanai waves at a period of about 17 days characterized by fluctuations in meridional velocity at the equator and in subsurface temperature at 2°N and 2°S. The fact that two waves have comparable wavelength indicates the 17-day wave near the equator travels much faster than the 33-day wave centered near 5°N. While the 33-day waves are identified as unstable first meridional mode Rossby wave, the 17-day wave did not show up as unstable waves when the authors ran a linearized model with five vertical modes and gradually increased the shear of the mean equatorial currents. Nonlinear model by Donohue and Wimbush (1998) generated a 15-day wave with a phase speed about 0.88 m/s with a strong meridional signal centered on the equator and a 30-day wave with a phase speed about 0.42 m/s with sea level maxima near 6°N. The authors argued that the 15-day wave arose from barotropic instability of the cyclonic shear of south flank of SECN while the 30-day waves arose from the barotropic instability of the anticyclonic shear of the north flank of SECN and baroclinic conversion near the core of SEC. Other nonlinear models by Mccreary and YU (1992) and Yu et al. (1995) also produced two waves with distinct periods (wave 1 with periods about 20 days and wave 2 with period about 40-50 days in their cases). However, close look indicates these two waves are nearly phase locked. So how these 17-20 day waves near the equator with relative fast propagating speed are generated still remains unclear.

* email: zhouc@umich.edu

The current paper also evaluates how the external forcings, like wind stresses, affect the nonlinear evolution of TIWs and examine whether secondary instabilities exist when the TIWs evolve to nonlinear vortices.

2. MODEL

Linearized Shallow-water Equations (SWEs) are used for the stability analysis of TIWs and full nonlinear SWEs to study the nonlinear evolution of TIWs. The shallow water model is also called 'the one-and-a-half-layer' model because it describes two-layer fluid in the hydrostatic approximation when the lower layer is infinitely deep.

3. RESULTS OF LINEAR STABILITY ANALYSIS

Linear stability analysis of barotropic Tropical Instability Waves(TIWs) are studied using various mean states from both Pacific and Atlantic oceans, see Figure 1 (left). The dependence of the properties(wavelength, period, and growth rate expressed in e-folding time) of the most unstable modes is studied by changing all three independent parameters (shear scale *L*, velocity magnitude *U* and equivalent depth *H*) which control the linearized shallow-water equations. Wavelengths are mainly determined by the shear scale L and U; periods are mainly determined by the velocity magnitude U; the e-folding times are most sensitive to L/U and can be approximated as an exponentially growing function of L/U, see Figure 2. Changing equivalent depth H only changes these properties slightly.

4. NONLINEAR EVOLUTION

4.1 FREE NONLINEAR EVOLUTION

The nonlinear evolution of TIWs is initialized with small perturbation to the initial mean states. During the early stages, the TIWs centered at about 5°N with periods about one month and a wavelength of about 1000 km dominate the whole domain. As these unstable TIWs grow into fully nonlinear vortices and stabilize the mean profile substantially, new waves with periods from 15-20 days are shown to emerge near the equator, see Figure 3. Meanwhile the initial unstable TIWs are slowed down and weakened. Stability analysis identifies the new appeared fast waves as neutral mixed Rossby-gravity(Yanai) waves, see Figure 4. The strength of these Yanai waves are sensitive to the initial mean flows. For moderately unstable initial means, they dominate from 3°S to 2°N. For strongly unstable initial means, they dominate from 7°S to 4°N. For weakly unstable means, they are weak and only appear closely on the equator.

4.2 FORCED NONLINEAR EVOLUTION

The effect of external forces (e.g. surface wind stress) is evaluated by simply adding nudging terms to the SWEs which act to nudge the flow back to the initial mean. Weak forcing terms, with a relaxation time of 90 days, have little effect on the TIWs development and appearance of the new Yanai waves during the first year but have huge effect in the long run by pushing the mean flow towards the initial mean significantly, helping TIWs near 5°N gain the dominance from 3°S to 7°N. Strong forcing terms, with a relaxation time of 30 days or less, can suppress the appearance of the fast Yanai waves.

4.3 SECONDARY INSTABILITY

We do not see any secondary instability within the vortices in all previous cases either due to the breakdown of the vortices or weak vortices. For weakly unstable case, the PV vortices are too weak. For moderately and strongly nonlinear cases, as the PV vortices grow to fully nonlinear stages and begin to rotate and expand in latitudinal direction. As a result, the initial PV vortices break down and stabilize the zonal mean substantially and also introduce the fast mixed Rossby-Gravity

waves which dominate near the equator. The reorganized reminiscent vortices near 5°N have relative uniform potential vorticity.

So to see secondary instability within a vortex, we need strong vortices which do not break after they begin to rotate. For theoretical purpose, we construct a case based on case PL550U07. First, we artificially introduce a reflection symmetry condition at the equator (surface height and u are symmetric about the equator and v is antisymmetric about the equator) to prevent the vortices expand across the equator and also prevent the formation of mixed Rossby-Gravity waves which are asymmetric across the equator. Second, we increase the velocity magnitude to 1.7 m/s. As a result, we successfully observed secondary instabilities after the PV vortices rotate and the gradient of PV intensify, see Figure 5. Secondary barotropic instability first appears in the outer region of the PV vortices and then in the core regions after two PV vortices merge.

5. CONCLUSION

Linear stability analysis shows that the wavelength of the most unstable mode depends on both shear scale L and U, the period depends mostly on U and e-folding time can be approximated as an exponentially growing function of L/U.

In nonlinear evolution, neutral Yanai waves are shown to appear after the most unstable TIWs grow to full nonlinear vortices and stabilize the zonal mean substantially. Meanwhile the vortices near 5°N are weakened and slowed down. External forcing terms help the initial TIWs dominate near 5°N and could suppress the appearance of the fast Yanai waves when these forcing terms are strong. Secondary barotropic instability within the vortices is possible when we apply reflection symmetric condition at the equator and increase the magnitude of the zonal mean.

6. REFERENCE

Chelton, D., F. Wentz, C. Gentemann, R. de Szoeke, and M. Schlax (2000), Satellite microwave SST observations of transequatorial tropical instability waves, *Geophysical Research Letters*, 27 (9), 1239-1242.

Chelton, D., S. Esbensen, G. Schlax, N. Thum, M. Freilich, F. Wentz, C. Gentemann, M. McPhaden, and P. Schopf (2001), Observations of coupling between surface wind stress and sea surface temperature in the eastern tropical Pacific, *Journal of Climate*, 14 (7), 1479-1498.

Donohue, K., and M. Wimbush (1998), Model results of flow instabilities in the tropical Pacific Ocean, *Journal of Geophysical Research-Oceans*, 103 (C10), 21, 401-21, 412.

Flament, P., S. Kennan, R. Knox, P. Niiler, and R. Bernstein (1996), The three-dimensional structure of an upper ocean vortex in the tropical Pacific Ocean, *NATURE*, 383 (6601), 610-613.

Halpern, D., R. Knox, and D. Luther (1988), Observations of 20-day period meridional current oscillations in the upper ocean along the pacific equator, *Journal of Physical Oceanography*, 18 (11), 1514-1534.

Jochum, M., P. Malanotte-Rizzoli, and A. Busalacchi (2004), Tropical instability waves in the Atlantic ocean, *Ocean Modelling*, 7 (1-2), 145-163.

Kennan, S., and P. Flament (2000), Observations of a tropical instability vortex, *Journal of Physical Oceanography*, 30 (9), 2277-2301.

Legeckis, R. (1977), Long waves in eastern equatorial Pacific ocean - view from a geostationary satellite, *Science*, 197 (4309),

1179-1181.

Lyman, J. M., G. C. Johnson, and W. S. Kessler (2007), Distinct 17-and 33-day tropical instability waves in subsurface observations, *Journal of Physical Oceanography*, 37 (4), 855-872.

Mccreary, J., and Z. YU (1992), Equatorial dynamics in a 2-1/2-layer model, *Progress In Oceanography*, 29 (1), 61-132.

Philander, S. G. H. (1978), Instabilities of zonal equatorial currents, 2, *J. Geophys. Res*., 83, 3679{3682.

Qiao, L., and R. Weisberg (1995), Tropical instability wave kinematics – observations from the tropical instability wave experiment, *Journal Of Geophysical Research-Oceans*, 100 (C5), 8677-8693.

Yu, Z., J. McCreary, and J. Proehl (1995), Meridional asymmetry and energetics of tropical instability waves, *Journal of Physical Oceanography*, 25 (12), 2997-3007.

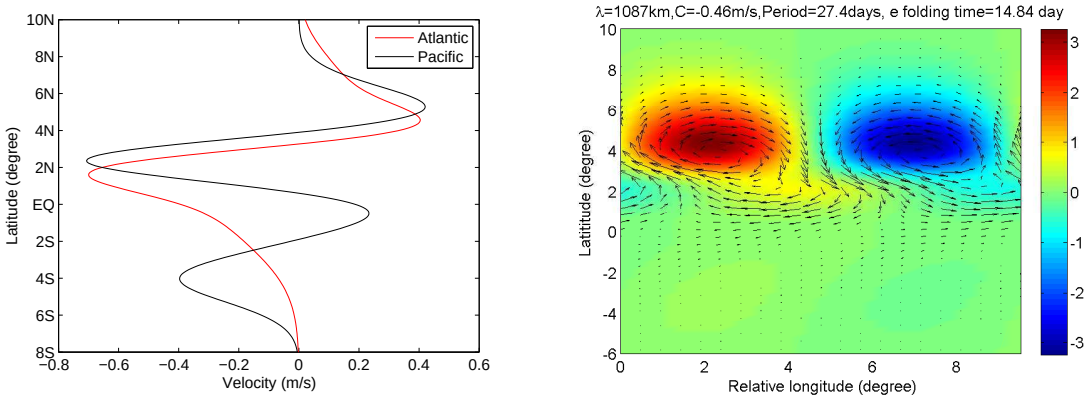

Figure 1 Left: Two typical surface mean states from the Atlantic (after Philander(1978)) and Pacific(after Hansen and Paul (1984)) oceans. We name these two profiles AL550U07 and PL550U07 where A and P denote Atlantic and Pacific, L is the approximate distance from the equator to the center of NECC (about 550 km for these two profiles), U is the maximum magnitude of the velocity(0.7 m/s for these two profiles). Variants of these two profiles are obtained by scaling L and U to a wider range. Right: The fastest growing mode of AL550U07. Background color represents the surface height with velocity field overlapped.

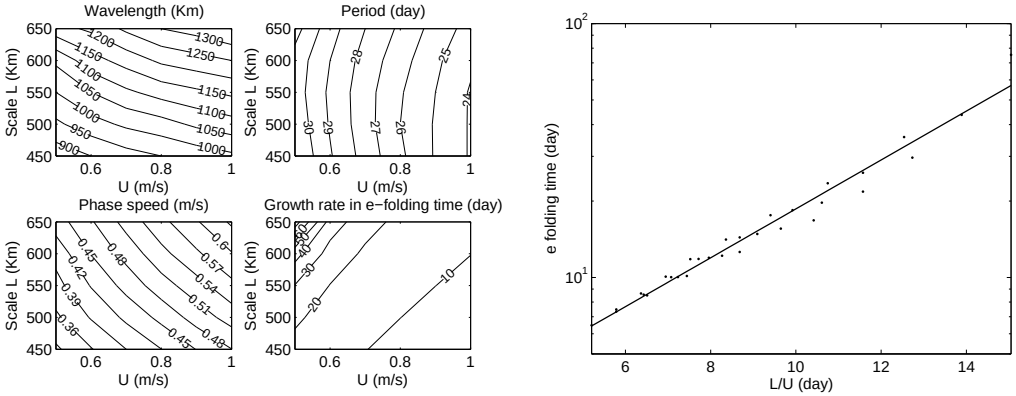

Figure 2 Left: Wavelength, period, phase speed and growth rate of the fastest growing modes of the mean states with different L and U in the Atlantic Ocean. An equivalent height of 0.5 m is used. Right: e-folding time versus L/U for profiles in the Atlantic Ocean. The solid line is a guide line. e-folding time increases approximately exponentially with L/U.

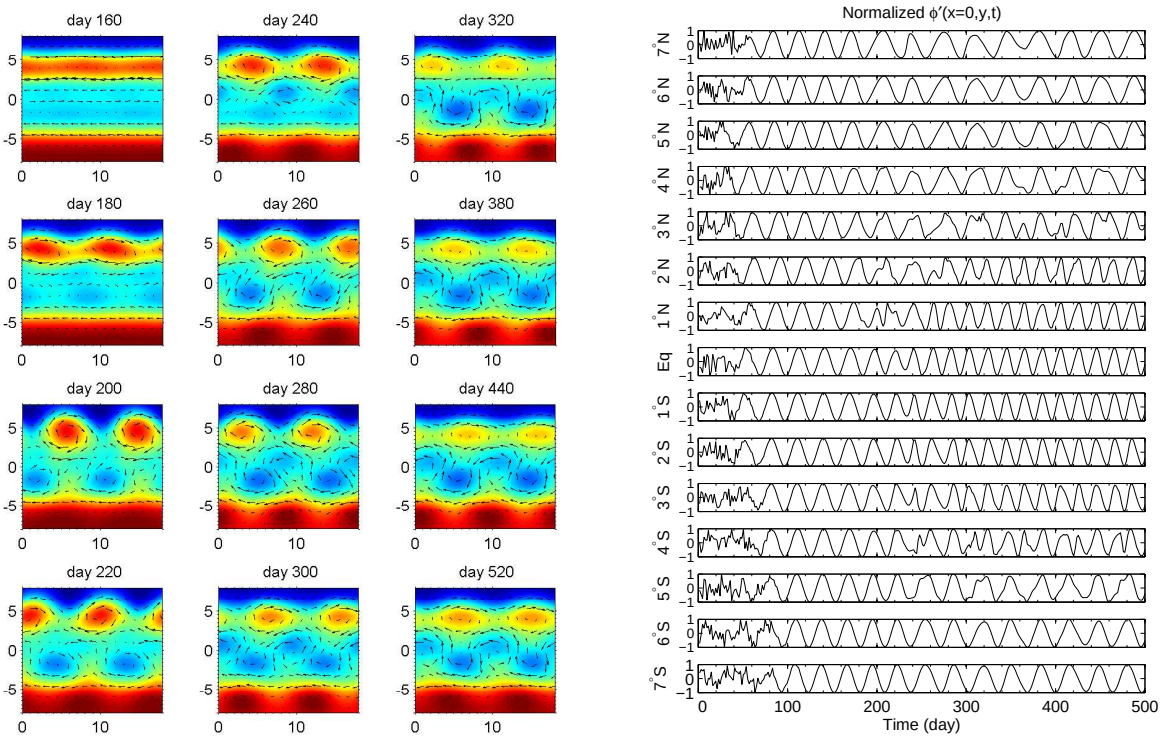

Figure 3 Left: Time evolution of surface height and velocity field of case PL550U07, x axis is the longitude in degree and yx axis is the latitude in degree. Right: Time evolution of normalized deviation of surface height Φ at different latitudes. Normalized deviation of surface height Φ the deviation of Φ at $x=0$ from its zonal mean divided by the maximum magnitude of all deviation of Φ along the latitude. Note that between 3°S and 2°N f ast waves with periods about 20 days appear after day 200.

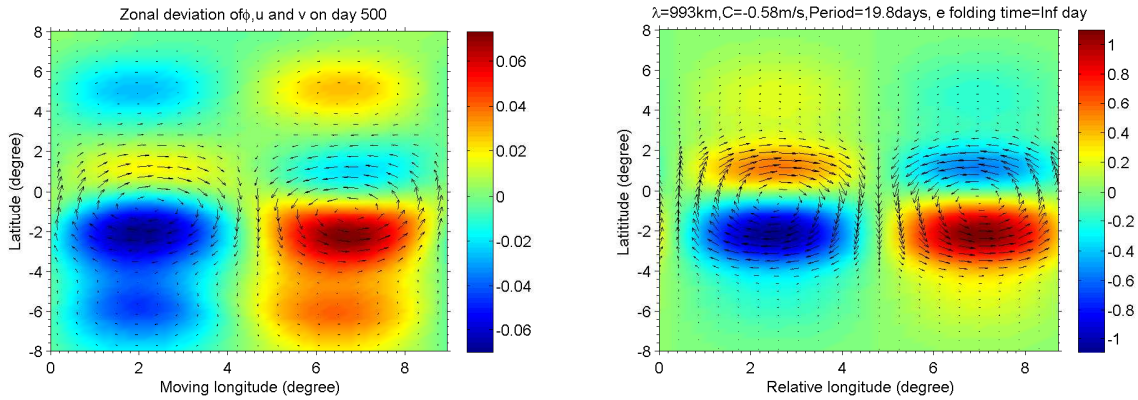

Figure 4 Left zonal deviation of Φ and u-v on day 500 of case PL550U07. Right: Neutral modified Yanai wave of the same wavelength from the stability analysis using the stabilized zonal mean.

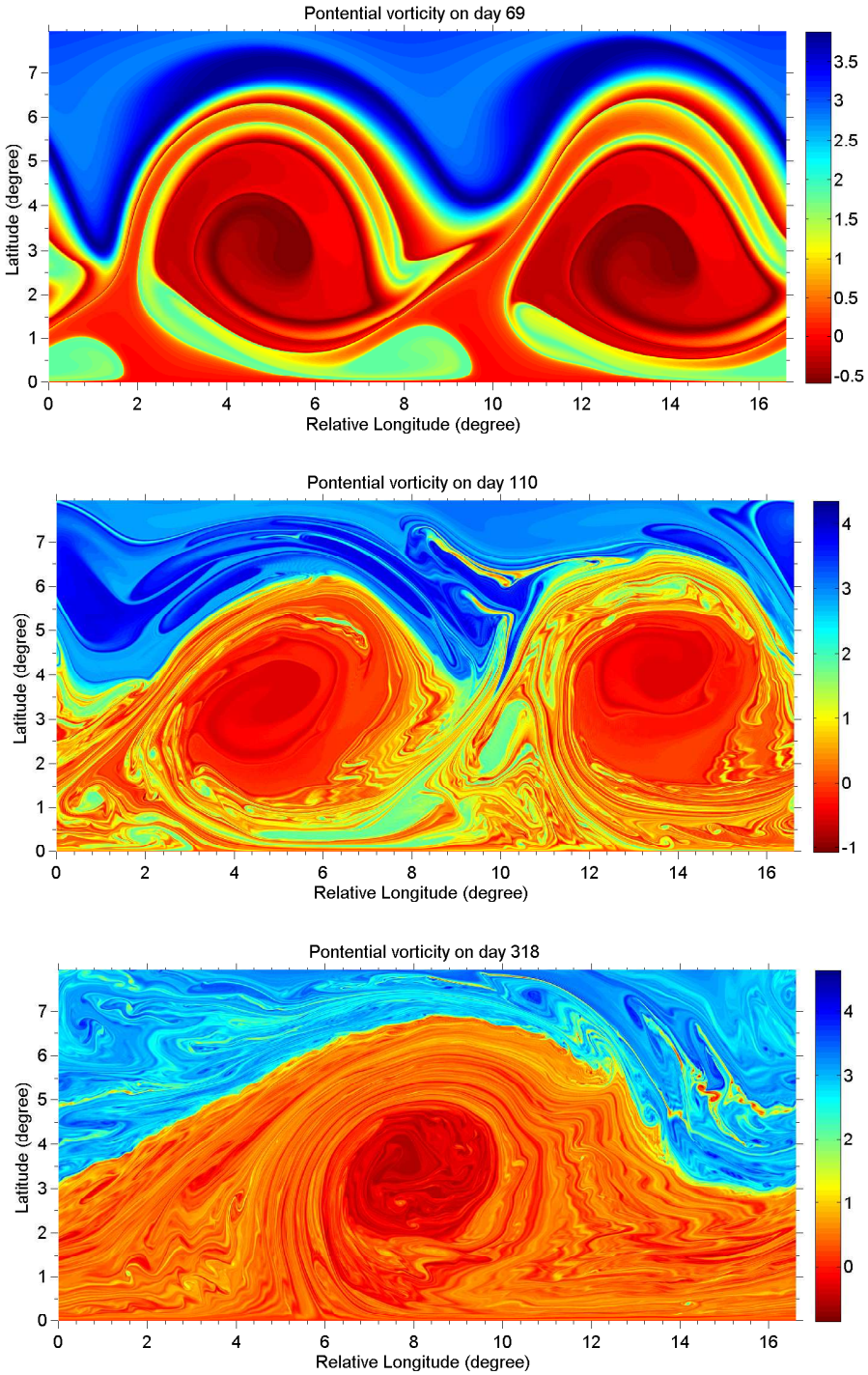

Figure 5 Potential vorticity on day 69 (top panel), day 110 (middle panel) and day 318 (bottom panel) for case PL550U17 when applying reflection symmetric condition at the equator. Note that there is no secondary instability on day 69. Secondary bartorpic instability appears in the outer regions of the PV vortices on day 110 and also in the core regions after two PV vortices merge.